Short communication

Ultrahigh activity of Pd decorated Ir/C catalyst for formic acid electro-oxidation

CrossMark

Jinwei Chen [a], Yuanjie Li [b], Zichen Gao [a], Gang Wang [a], Jing Tian [a], Chunping Jiang [a]
, Shifu Zhu [a], Ruilin Wang [a],*

[a] College of Materials Science and Engineering, Sichuan University, Chengdu 610065, China
[b] Central Research Academy of Dongfang Electric Corporation, Chengdu 611731, China

ARTICLE INFO

ABSTRACT

A core–shell like Ir/C@Pd catalyst with ultrahigh activity toward formic acid electro-oxidation (FAEO) was prepared by decorating Pd shell on the Ir NPs for the first time. The structure has been demonstrated by XRD, XPS, TEM, EDS and electrochemical techniques. The mass-normalized current density at 0.08 V (vs. SCE) of Ir/C@Pd for FAEO is 3756 mA mg$^{-1}_{Pd}$, which is about 3.38 and 4.16 times higher than that of the PdIr/C and commercial Pd/C, respectively. The remarkable performance of Ir/C@Pd should be attributed to its unique core–shell like structure and the enhanced electronic coupling between the Ir and Pd, which was confirmed by XPS results.

© 2013 Elsevier B.V. All rights reserved.

1. Introduction

Direct formic acid fuel cells (DFAFCs) have been investigated as an alternative to direct methanol fuel cells (DMFCs) for portable power applications [1–5]. Palladium (Pd) catalysts [6–10] have been well studied for their superior electrochemical activity toward FAEO. However, it suffers from long term durability issues. In order to further improve the activity and durability of Pd catalysts, the Pd–M (M = Co [11], Cu [12] and Ni [13]) alloy catalysts with enhanced performance have been investigated. Wang et al. [14] reported for the first time that the PdIr/C catalyst showed a better activity and durability for FAEO than the Pd/C catalyst because of the electronic effect and the bi-functional mechanism of Ir to Pd. We [15] also have prepared the PdIr/C catalyst by an ethylene glycol (EG)-assisted NaBH$_4$ reduction method [16] and optimized the mass ration of Pd to Ir. The activity is much higher than the previous work [14].

Recently, another effective method of enhancing catalytic activity is the core–shell construction of nanosized bimetallic particles. Arranging noble metal as thin (ideally monolayer) shells on proper non-noble metal core (denoted as core@shell) not only reduces their usage, but also could significantly enhance their catalytic performance by the so-called strain and ligand effect of the core substrate on the supported noble metal overlayer. Core–shell structure catalysts, such as Au@Pt [5] and Au@Pd [17], have been investigated for FAEO and showed

enhanced electrocatalytic activity and durability. However, to the best of our knowledge, the core–shell structure PdIr bimetallic catalyst for FAEO has not been reported yet.

Based on the foregoing, we fabricated core–shell like PdIr catalyst by decorating Ir nanoparticles (NPs) with a Pd shell via a two-stage route. Then, the performance of the prepared Ir/C@Pd catalyst for FAEO was evaluated.

2. Experimental

The synthesis of Ir/C@Pd (20 wt.% of metal loading) catalyst started from preparing carbon supported Ir NPs using our developed EG-assisted NaBH$_4$ reduction method [16]. Briefly, 40 mg of pretreated carbon black and appropriate H$_2$IrCl$_6$ aqueous solution were dispersed in 20 ml EG with stirring for 1.0 h. A freshly prepared NaBH$_4$ in EG solution was added dropwise into the above solution at 20 °C and the resulting suspension was stirred for 1.0 h. The product was filtered, washed, and dried in a vacuum oven at 75 °C. To form Pd shell, appropriate PdCl$_2$ was dissolved in 20 ml EG. The obtained powder of Ir/C was submitted to the flask (Pd:Ir = 7:3 in atomic ratio). Then, the reduction of Pd and the collection of product are the same as the above procedure. For comparison, PdIr/C and Pd/C catalysts were prepared using the same reduction approach and the PdIr was co-reduced by one-stage route, and a commercial Pd/C catalyst also was purchased from Sigma-Aldrich.

XRD, XPS, TEM and EDS were used to analyze the structure, surface information and morphology of the prepared catalysts. All electrochemical measurements were carried out in a conventional three-electrode electrochemical cell using cyclic voltammetry (CV) and chronoamperometry

(CA) techniques. The counter electrode was a graphite electrode and the reference electrode was a saturated calomel electrode (SCE). All potentials reported in this paper were referred to the SCE. A glassy-carbon working electrode was used as substrate. The calculated loading of metal was 35 μg cm^{-2}. The CVs were carried out in an Ar-saturated solution of 0.5 M H_2SO_4 without or with 0.5 M HCOOH. The CAs were carried out under a magnetic stirring condition with the same speed to eliminating the bubbles on the working electrode surface.

3. Results and discussion

Fig. 1 shows the XRD patterns of the prepared Ir/C@Pd, PdIr/C and Pd/C catalysts. The first peak located at about 24.8° in all the XRD patterns is associated to the (002) diffraction of the carbon support. The other diffraction peaks of homemade Pd/C catalyst [curve (c)] at 39.3°, 45.8°, 66.8° and 80.4° correspond to the (111), (200), (220) and (311) crystal planes of Pd (ICSD#: 64918) with a face-centered cubic lattice structure. From the curves (a) and (b), it can be observed that the Ir/C@Pd and PdIr/C catalysts also show the Pd fcc lattice structure, but a positive shift of the Pd peaks occurs obviously, indicating that the Ir atoms enter into the Pd crystals. The average crystallite sizes of the prepared Ir/C@Pd, PdIr/C and Pd/C catalysts are estimated to be about 3.0 nm, 2.6 nm and 3.2 nm using the Scherrer equation [18].

Fig. 2 shows the XPS spectra. It can be observed from the wide-scan XPS spectra that all the Ir/C@Pd and PdIr/C catalysts have Ir 4f spectra, which means that Ir was detected on the surface of Ir/C@Pd catalyst. The results from SEM-EDS (not presented here) also showed the existence of Ir. It should be demonstrated that the Pd shell is too thin or the prepared Ir/C@Pd catalyst shows incomplete core–shell structure. However, the detected atomic ratio of Ir peak in Ir/C@Pd [the inset (B) in Fig. 2] is obviously much lower than that of PdIr/C, demonstrating that the surface of Ir@Pd is enriched by Pd. Moreover, from the inset (A) in Fig. 2, curve (c) reveals the presence of Pd $3d_{5/2}$ and $3d_{3/2}$ peaks ant binding energy of 335.0 and 340.3 eV, respectively. The binding energy of Pd $3d_{5/2}$ in all the Pd–Ir NPs slightly shifts to higher energy compared to the sole Pd. Ir/C@Pd with $\triangle E = 0.25$ eV shows the largest binding energy shift while that of PdIr/C is only 0.09 eV. The shift of binding energy implies surface electronic modification of the Pd resulting from the interaction with the Ir.

The structure and morphology of Ir/C@Pd were further characterized by TEM as shown in Fig. 3. It is observed that a large number of small NPs are highly dispersed on the carbon support. Some of metal particles clearly display the Ir core and Pd shell formed by the contrast due to different atomic weights. Most of the Ir@Pd NPs on the carbon support have a diameter range from 2 to 5 nm, and the average size was measured to be about 4.0 nm. Moreover, the HRTEM image describing the crystalline nature of Ir@Pd NPs is shown in Fig. 3(b). The single
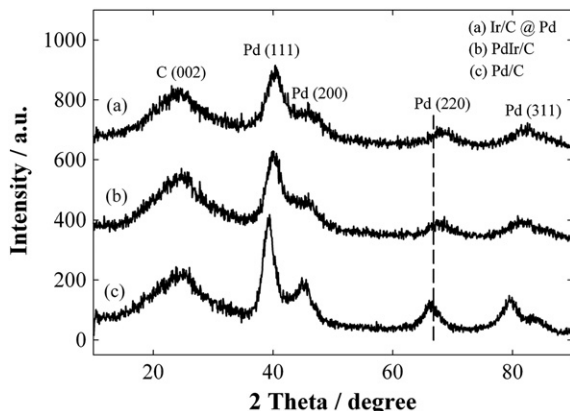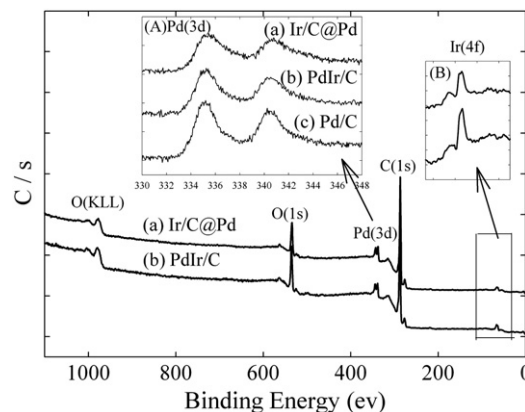

Fig. 2. XPS survey spectra of the (a) Ir/C@Pd and (b) PdIr/C catalysts. The insert (A) and (B) show the Pd 3d and Ir 4f core level XPS spectra of the catalysts, respectively.

crystalline of Ir@Pd particles are confirmed, the lattice planes with inter layer distance of 0.218 nm in the core are indexed to Ir(111) crystal planes, the outer layers with the lattice space of 0.227 and 0.230 nm correspond to Pd(111) crystal planes. It demonstrates island-like Pd domains at the Ir surface.

The electrochemical characteristics of catalysts were evaluated by CV and shown in Fig. 4. The CV curves in Fig. 4(a) were obtained in 0.5 M H_2SO_4 solution without formic acid. The catalysts exhibit hydrogen adsorption/desorption peaks in the potential region of -0.2 V to 0 V. Although the average particle size of PdIr/C catalyst is the smallest, the current of hydrogen adsorption/desorption peaks is the lowest. It should be attributed to the existence of PdIr alloy phase in PdIr/C catalyst. However, the Ir/C@Pd catalyst has the highest current of hydrogen adsorption/desorption even if it has larger average particles. It should be explained that the island-like Pd NPs with small size covered the Ir surface, which resulted in the large electrochemical active surface area (EASA). This should be another evidence for the core–shell like structure of the Ir@Pd NPs.

Fig. 4(b) shows CVs (only present forward scan curves) of the four samples for FAEO. It is observed that the peak potential of FAEO on the Pd/C catalysts are almost the same, while the current density (normalized to the mass of Pd loading) of homemade Pd/C is slightly higher than commercial Pd/C (1458 mA mg^{-1}$_{Pd}$ vs. 1244 mA mg^{-1}$_{Pd}$). The peak potential of PdIr/C catalyst shows a biggish negative shift (150 mV) compared to that of Pd/C. And the PdIr/C catalyst exhibits higher current density in the potential region of -0.12 V to 0.8 V than that of Pd/C catalysts. These should be attributed to the electronic effect and the bi-functional mechanism of Ir to Pd. However, the core–shell like Ir/C@Pd catalyst clearly shows superior activity to other catalysts. The onset potential of FAEO on the Ir/C@Pd catalyst is -0.18 V, which is more negative than that of other catalysts. And the potential and current density of forward anodic peak are 0.08 V and 3756 mA mg^{-1}$_{Pd}$, respectively. The mass activity of the Ir/C@Pd catalyst at 0.08 V is about 3.38 and 4.16 times higher than that of the PdIr/C and commercial Pd/C, respectively. Even if the current densities were normalized to the mass of metal loading [Fig. 4(c)], the Ir/C@Pd catalyst also shows the highest catalytic activity. To further investigate the activity and stability of the catalysts, CA curves on the four samples toward FAEO were conducted at 0.15 V for a period of time, as shown in Fig. 4(d). In the region of activation polarization, the Ir/C@Pd exhibits the highest current density, and its final current density is 502 mA mg^{-1}$_{Pd}$ compared with 31,238 and 92 mA mg^{-1}$_{Pd}$ obtained for PdIr/C, homemade Pd/C and commercial Pd/C. The remarkable electrocatalytic activity enhancements should be attributed to the unique core–shell like structure of Ir@Pd NPs which results in the larger EASA and the stronger electronic coupling between Ir and Pd than that of the co-reduced PdIr NPs.

Fig. 1. XRD patterns of the (a) Ir/C@Pd, (b) PdIr/C and (c) Pd/C catalysts.